鹿林天文台 CCD 光度系統之特性與效能

木下大輔[1,2,*]、陳錦威[1]、林宏欽[1]、林忠義[1]、黃癸雲[1]、張永欣[1]、陳文屏[1]

[1] 國立中央大學天文研究所

[2] 日本國立天文台

摘要

台灣鹿林天文台光學一米望遠鏡於 2003 年一月起正式開放於科學觀測。爲了評估 CCD 光度系統的效能和特性，我們從 2004 年二月至四月觀測許多藍道(Landolt)標準星做爲光度校正的指標。在此文章，我們報告整個系統的初步分析結果，其內容包括了"CCD 的增益值、讀出噪音、暗電流效應、標準濾鏡 UBVRI 的轉換係數（大氣消光係數、色指數和極限星等值）與天光背景的亮度"等。

Characteristics and Performance of the CCD Photometric System at Lulin Observatory

Kinoshita Daisuke[1,2], Chen Chin-Wei[1], Lin Hung-Chin[1], Lin Zhong-Yi[1], Huang Kui-Yun [1], Chang Yung-Shin[1], Chen Wen-Ping[1]

[1] Institute of Astronomy, National Central University

[2] National Astronomical Observatory of Japan

Abstract

The Lulin One-meter Telescope at Lulin Observatory in Taiwan started the open-use observations in January 2003. In order to evaluate the performance of the CCD photometric system and the characteristics and quality of the site, we have obtained the data of photometric standards as well as calibration data from February to November 2004. We report the results of our analysis including gain, readout noise, dark current and linearity of the CCD, transformation coefficients, total throughtputs, night sky brightnesses and limiting magnitudes for UBVRI bands.

關鍵字（Key words）：電子耦合元件（CCD）、校正（calibration）、轉換係數（transformation coefficients）

* Offprint request should be sent to kinoshita@astro.ncu.edu.tw

1. Introduction

The Lulin One-meter Telescope (hereafter, LOT) was installed at the summit of Mount Lulin (120º 52' 25" E, 23º 28' 7" N, H = 2862 m) in the central region of Taiwan by the Institute of Astronomy of National Central University in September 2002. After three months of test observations, the open-use observations have begun in January 2003 (Chang, 2004). It is essential to know the properties and performance of the instrument to conduct scientific observations. We have started a program to evaluate the characteristics of CCD photometric system on LOT in November 2003. Here, we report the results of our analysis of the performance of the CCD photometric system and the characteristics and the qualities of the site. We introduce briefly about the instrument in section 2, report the basic characteristics of the CCD in section 3, give the transformation coefficients in section 4, and show the total system performances in section 5, and summarize in section 6.

2. Instrument

The LOT is a telescope with an effective diameter of 1000 mm. The CCD imaging camera is attached to the Cassegrain focus of the telescope. At the beginning of the open-use observations, the CCD camera "AP8" manufactured by Apogee, Inc. was used. In June 2003, the operation of CCD camera "VersArray:1300B" manu factured by Princeton Instruments, Inc. was started. Since AP8 was retired in January 2004, here we concentrate on the performance of the VersArray:1300B. The performance of the AP8 CCD photometric system was reported by Kinoshita et al. (2004).

The specifications of the CCD camera VersArray:1300B is summarized in Table 1 (Princeton Instruments, Inc., 2004). The telescope focal length is 8000 mm, resulting in a pixel scale of 0.516 arcsec per pixel. This is reasonably spatially sampled under the typical seeing of 1.5 arcsec at Lulin Observatory. The field of view of this system is 11.5 arcmin by 11.2 arcmin. The CCD is cooled by thermoelectric cooling together with water circulation. The typical operation temperature is -50ºC. The data acquisition is done using the software "Maxim DL" provided by the Diffraction Limited, Inc. running on Windows operating system. The data are recorded on the SAMBA shared file system on Linux operating system.

Table 1.Specifications of the CCD camera VersArray:1300B as provided from Roper Scientific, Inc. are summarized

CCD Chip	EEV CCD36-40 (back-side illuminated)
Pixel Number	1340 × 1300
Pixel Size	20 μm× 20 μm
Imaging Area	26.8 mm × 26.0 mm
CCD Grade	Scientific Grade; Grade 1
Full Well	200,000
AD Conversion	16 bits
Sampling	50 kHz (slow mode) 1 MHz (fast mode)
Readout	36 sec @ 50 kHz 1.8 sec @ 1 MHz
Read Noise	3 e^- rms @ 50 kHz 10 e^- rrms @ 1 MHz
Dark Current	0.1 e^-/pixel/sec @ -40ºC 0.5 e^-/pixel/hr @ -110ºC

3. Performance of the CCD

3.1 Bias

The mean bias level is about 89 ADU (Analog-to-Digital Unit) for slow readout mode, and about 150 ADU for fast readout mode. The

readout time of fast readout mode is less than two seconds, and the efficiency of data acquisition is very high. This mode is powerful especially for taking flatfields during the twilight. Figure 1 and 2 show the stability of mean bias levels for slow and fast readout modes, respectively. It seems the mean bias level of fast readout mode is correlated with ambient temperature, and changes more than 15 ADU within a day. One of the explanations is the stray light causing the increase of the bias level after the sunrise in the morning. However, the stray light cannot explain the gradual decrease at night. We need further investigations of this phenomenon. Because of this instability, it is encouraged to take bias frames often during the night to monitor the variability for high precision photometry when fast readout mode is used.

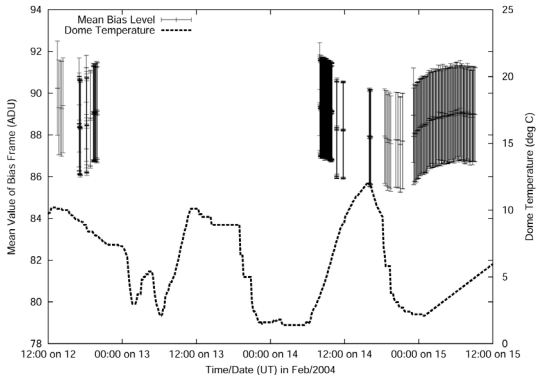

Fig 1. he level of bias frame is plotted against data acquisition time in UT. The data are taken under the slow readout mode.

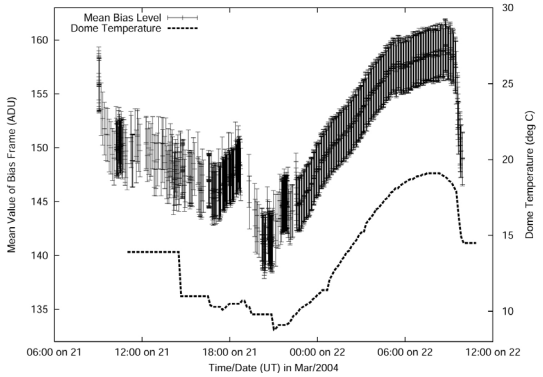

Fig 2. The level of bias frame is plotted against data acquisition time in UT. The data are taken under the fast readout mode. The ambient temperature in the dome of LOT is also shown as the dotted line.

3.2 Gain and Readout Noise

The gain G is the conversion factor of how many electrons are required to produce a digital number for the output data. The number of electrons is expressed as

$$n_e = G n_{ADU} \quad (1)$$

Here, n_e is the number of electrons, n_{ADU} is the Analog-to-Digital Unit (ADU), and G (e^-/ADU) is the gain. The standard deviation of the difference between two flatfield images $\sigma_{F1\text{-}F2}$ contains Poisson noise in addition to the readout noise (Howell, 2000),

$$\sigma^2_{F_1-F_2} = 2\left\{\left(\frac{\sqrt{n_e}}{G}\right)^2 + \left(\frac{R}{G}\right)^2\right\} \quad (2)$$

Here, $R(e^-)$ is the readout noise. Subtracting two flatfield images increases the noise by a factor of $\sqrt{2}$. Hence, the relationship between the signal S and the noise N is expressed as

$$N = \sqrt{\frac{S}{G} + \left(\frac{R}{G}\right)^2} \quad (3)$$

We took images of flatfield using a white screen in the dome. We used both broad- and narrow-band filters to cover a wide range of signal levels. We used B for the broad-band filter and CN for the narrow-band filter. The integration times were set from 3 to 60 sec. For each integration time, five frames were continuously taken. We tested both the fast readout mode of 1 MHz sampling and slow readout mode of 50 kHz sampling. Basically we follow the method described by Motohara et al. (2002). All the measurements were carried out under the cooling temperature of -50ºC. Since we took five frames for each signal level, we made ten pairs of two frames from five frames. For each pair of images, we subtracted one from another, and measured the standard deviation. We divided the standard

deviation by $\sqrt{2}$ to derive the noise level. We also subtracted combined dark frame from flatfield images to measure the mean signal level of the flatfields to derive the signal level. To check the uniformity of the properties of the CCD, we divided the CCD into four regions. Here, we call the 301 ≤ x ≤ 600, 301 ≤ y ≤ 600 region of the image "Region A", 301 ≤ x ≤ 600, 701 ≤ y ≤ 1000 "Region B", 701 ≤ x ≤ 1000, 301 ≤ y ≤ 600 "Region C", and 701 ≤e x ≤ 1000, 701 ≤ y ≤ 1000 "Region D". The alignment of four regions are shown in Figure 3. The signal and the noise were measured for all four regions.

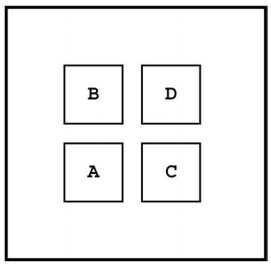

Fig 3. The schematic view of the alignment of four subregions for gain measurements on the CCD. All subregions have 300 by 300 pixels.

The results of the measurements for the fast and slow readout modes are shown in Figure 4 and 5, respectively. We fitted the measurements with Equation (3). The gain G is 3.0 e^-/ADU for all four regions for fast readout mode, and is 2.0 e^-/ADU for all four regions for slow readout mode. The readout noise is 7.1-7.4 e^- for fast readout mode, and 4.4-4.5 e^- for slow readout mode.

Table 2. The dark current generation rates are shown. The second column shows the readout mode. The word "slow" denotes 50 kHz sampling, and ``fast'' denotes 1 MHz sampling. The third column shows the operating temperature of the CCD. The dark current generation rate is expressed in number of electrons per second per pixel.

Date	Readout	Temp. (deg C)	Dark Current (e^{-1}/sec/pix)
13/Feb/2004	fast	-50	0.063
24/May/2004	slow	-50	0.067
25/May/2004	fast	-50	0.065
26/May/2004	fast	-50	0.055
22/Jun/2004	slow	-50	0.065
23/Jun/2004	slow	-50	0.073
24/Jun/2004	slow	-50	0.065
25/Jun/2004	slow	-50	0.057
16/Aug/2004	slow	-50	0.059
17/Aug/2004	slow	-50	0.070

3.3 Dark Current

The dark frames with different integration times were obtained to estimate the dark current generation rate. The results are summarized in Table 2. The average value shows 0.064 e^-/sec/pix for the operation temperature of -50 deg C.

3.4 Linearity

In order to check the linearity of the response of the CCD, we have carried out a measurement using camera lens and LEDs. We placed eight LEDs in the sphere. We attached the camera lens to the CCD and located the CCD at small hole of the sphere. We imaged inside of the sphere for various exposure time ranging 5 to 80 seconds. For each exposure time, we took 5 frames. The measurements are done using slow readout mode, and the dark component is subtracted. Figure 6 shows the mean count of 100 × 100 pixels near the center of the field against exposure time. We fitted the data with the formula

$$C = at^{\gamma} + b \qquad (4)$$

Here, C is the mean count, t is the exposure time, a, b and γ are constants. The deviation from $\gamma = 1$ was 0.1% for the range from 3000 to 38000 ADU. The non-linearity degraded to 1.7% when the mean count reached 51000 counts.

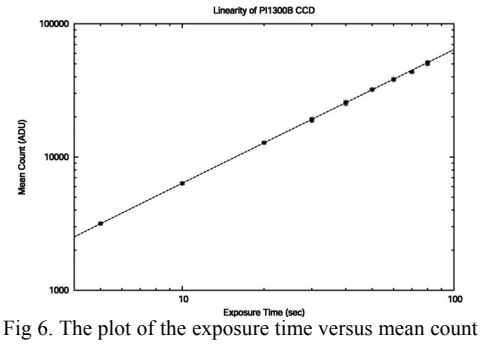

Fig 6. The plot of the exposure time versus mean count of the CCD is shown. The light source is eight LEDs. The dotted line is the fit using equation (4).

4. Photometric Calibrations

In order to compare the results of the photometry with the results from other instruments, one needs to convert the magnitudes from the instrumental system into the standard system. To achieve this conversion, it is essential to evaluate the transformation coefficients. Here, we define transformation equations as

$$U_{std} = U_{inst} + Z_U - k_u X + C_u(U-B) \quad (5)$$

$$B_{std} = B_{inst} + Z_B - k_B X + C_B(B-V) \quad (6)$$

$$V_{std} = V_{inst} + Z_V - k_V X + C_V(B-V) \quad (7)$$

$$R_{std} = R_{inst} + Z_R - k_R X + C_R(V-R) \quad (8)$$

$$I_{std} = I_{inst} + Z_I - k_I X + C_I(V-I) \quad (9)$$

where U_{std}, B_{std}, V_{std}, R_{std}, I_{std} are the standard magnitudes, U_{inst}, B_{inst}, V_{inst}, R_{inst}, I_{inst} are the instrumental magnitudes, Z_U, Z_B, Z_V, Z_R, Z_I are zero point magnitudes, k_U, k_B, k_V, k_R, k_I are the first-order extinction coefficients, C_U, C_B, C_V, C_R, C_I are the color terms, and X is the airmass. The net fluxes inside the aperture for standard stars are normalized to the exposure time of one second to calculate the instrumental magnitudes. We have chosen photometric standards from the list provided by Landolt (1992) to cover a wide range of colors and airmass. We have used UBVRI filters. The BVRI filters are based on the Bessell system, and their transmission properties are reported by Huang et al. (2004). The property of the U-band filter is unknown and we are planning to measure the transmittance in the laboratory. Basically we used the "photcal" package of IRAF (Image Reduction and Analysis Facility, providec and maintained by NOAO) to fit the data and derive the coefficients. The values are confirmed by manual analysis using the method described by Henden and Kaitchuck (1990). The second-order extinction terms are found to be small and we ignored them. The results for seven different nights are summarized in Table

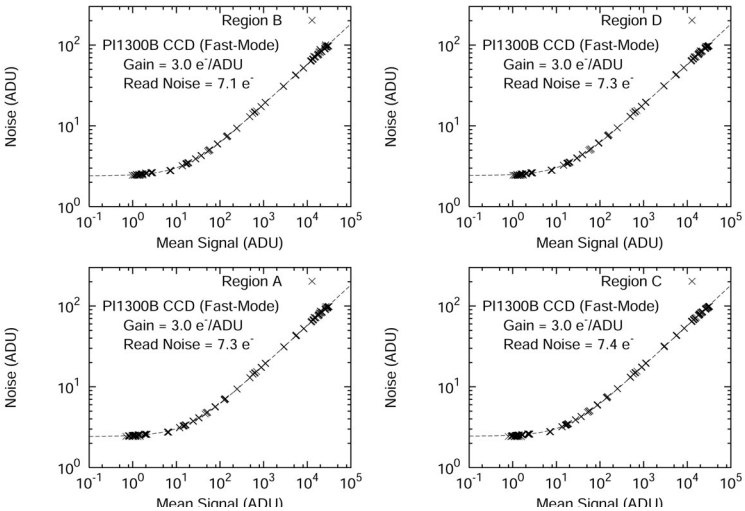

Fig 4. The signal and the noise of 300 × 300 regions on the CCD for fast readout mode are shown. The dotted curves are the fit using equation (3).

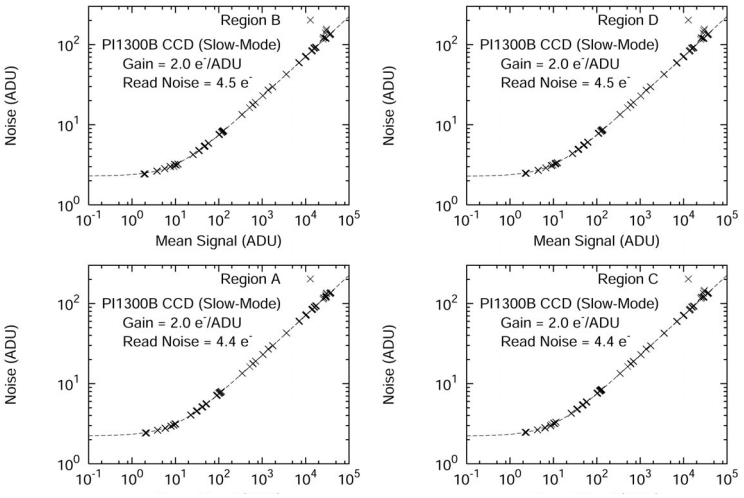

Fig 5. The signal and the noise of 300 × 300 regions on the CCD for slow readout mode are shown. The dotted curves are the fit using equation (3).

Table 3. The transformation coefficients including zero point magnitudes, first order extinction coefficients, and color terms of LOT and VersArray:1300B for UBVRI filters on seven different nights are summarized. The extinction coefficients are in the unit of magnitude per airmass. On 17 Feb 2004, the fast readout mode was used, and the zero point magnitudes are different from other nights. For other six nights, the slow readout mode was used.

	17/Feb/2004	19/Apr/2004	24/Jun/2004	25/Jun/2004	01/Sep/2004	09/Nov/2004	11/Nov/2004
Z_U	20.02± 0.03	20.20± 0.10	20.23± 0.05	20.28± 0.06			
Z_B	22.34± 0.02	22.83± 0.01	22.82± 0.02	22.81± 0.02	22.76± 0.08	22.70± 0.01	22.78±0.01
Z_V	22.68± 0.02	23.11± 0.01	23.11± 0.02	23.11± 0.01	23.06± 0.05	23.01± 0.01	23.09±0.03
Z_R	22.66± 0.01	23.07± 0.04	23.08± 0.02	23.10± 0.02	23.00± 0.02	22.96± 0.01	23.05±0.02
Z_I	21.99± 0.04		22.36± 0.03	22.43± 0.03	22.40± 0.03	22.30± 0.02	22.37±0.04
k_U	0.45 ± 0.01	0.46 ± 0.01	0.41 ± 0.02	0.41 ± 0.03			
k_B	0.19 ± 0.02	0.25 ± 0.01	0.24 ± 0.01	0.21 ± 0.01	0.22 ± 0.04	0.21 ± 0.01	0.20 ±0.01
k_V	0.11 ± 0.01	0.16 ± 0.01	0.16 ± 0.01	0.13 ± 0.01	0.10 ± 0.02	0.12 ± 0.01	0.12 ±0.01
k_R	0.09 ± 0.01	0.12 ± 0.01	0.13 ± 0.01	0.11 ± 0.01	0.05 ± 0.01	0.08 ± 0.01	0.09 ±0.01
k_I	0.06 ± 0.01		0.08 ± 0.03	0.08 ± 0.02	0.10 ± 0.02	0.06 ± 0.01	0.04 ±0.01
C_U	+0.15± 0.02	+0.30± 0.10	+0.32± 0.02	+0.32± 0.06			
C_B	+0.20± 0.02	+0.14± 0.01	+0.15± 0.01	+0.11± 0.02	+0.21± 0.03	+0.17± 0.01	+0.13±0.01
C_V	-0.06± 0.02	-0.06± 0.01	-0.06± 0.01	-0.08± 0.02	-0.05± 0.02	-0.07± 0.01	-0.10±0.03
C_R	-0.05± 0.02	-0.12± 0.05	-0.07± 0.02	-0.15± 0.03	-0.13± 0.01	-0.12± 0.02	-0.12±0.02
C_I	+0.04± 0.03		+0.05± 0.01	+0.04± 0.03	+0.07± 0.01	+0.03± 0.03	+0.00±0.03

Table 4. The atmospheric extinction coefficients for selected ground based astronomical observatories are summarized. The first order extinction coefficients for UBVRI bands are shown in the unit of mag per airmass. The numbers in the parenthesis are the errors.

Site	U	B	V	R	I	Ref.
Brooks	0.62 (0.09)	0.37 (0.07)	0.25 (0.04)	0.20(0.06)	0.14 (0.07)	Miller & Osborn, 1996
Gaomeigu			0.14			Tan & Zhang, 1999
Kiso		0.27 (0.02)	0.17 (0.01)	0.09 (0.01)	0.05(0.01)	Ito, 1998a
Kitt Peak			0.20 (0.01)		0.08 (0.02)	French et al., 1985
La Palma			0.11			Guerrero et al., 1998
La Silla		0.25	0.13	0.07	0.03	Mattila et al., 1996
La Silla	0.46	0.23	0.12			Nakos et al., 1997
Lulin	0.43 (0.02)	0.20 (0.02)	0.12 (0.01)	0.10 (0.01)	0.07 (0.02)	This work
Mauna Kea (2800-m)		0.31	0.18			Krisciunas et al.,1987
Mauna Kea (4200-m)		0.20	0.11			Krisciunas et al.,1987
Paranal	0.50 (0.03)	0.26 (0.01)	0.17 (0.01)	0.13(0.01)	0.07 (0.02)	Giacconi et al., 1999
Paranal	0.44 (0.01)	0.23 (0.01)	0.11 (0.01)	0.07(0.01)	0.03 (0.01)	Hanuschik, 2004
Siding Spring	0.54 (0.02)	0.31 (0.03)	0.16 (0.03)	0.11(0.02)	0.09 (0.03)	Sung & Bessell, 2000
Tololo	0.56	0.28	0.16	0.12		Stone & Baldwin, 1983
Xinglong	0.60	0.31	0.20	0.14	0.05	Yan etal., 2000

3. The plots of the Landolt magnitude versus calculated magnitude using derived transformation coefficients on 25 June, 2004 are shown in Figure 7 to 11. No systematic errors are recognized. The atmospheric extinction coefficients at various astronomical sites on the ground are summarized in Table 4. The extinction coefficients at Lulin Observatory on relatively dry nights are comparable to those of major ground based obesrvatories.

The instrumental colors are plotted against Landolt standard colors in Figure 12 to 16. From the linear fits, we have obtained the following relations,

$$(U\text{-}B) = 1.18\ (u\text{-}b) - 3.02, \quad (10)$$

$$(B\text{-}V) = 1.25\ (b\text{-}v) - 0.41, \quad (11)$$

$$(V\text{-}R) = 0.99\ (v\text{-}r) + 0.03, \quad (12)$$

$$(V\text{-}I) = 0.91\ (v\text{-}i) + 0.64, \quad (13)$$

$$(R\text{-}I) = 0.82\ (r\text{-}i) + 0.57. \quad (14)$$

Here, capital letters denote the standard system and small letters denote the instrumental system.

5. System Performance

5.1 System Efficiency

Using the photometric observations of the Landolt standard fields, we have estimated the

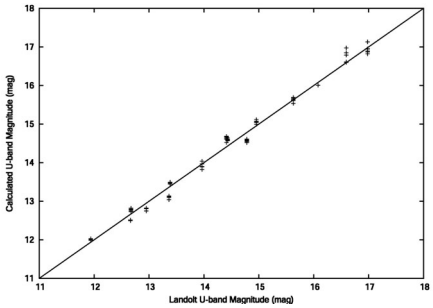

Fig7. The Landolt magnitude versus calculated magnitude using derived transformation coefficients for U-band are shown. The data taken on 25 June, 2004 are used to plot.

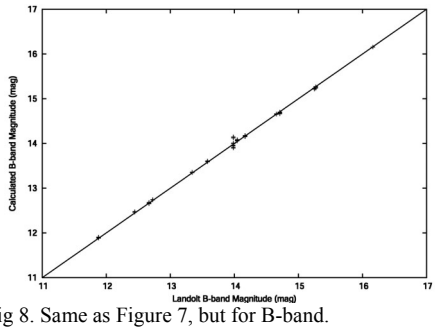

Fig 8. Same as Figure 7, but for B-band.

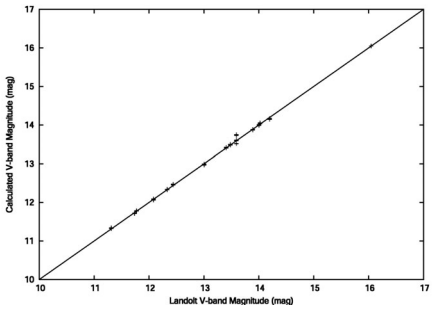

Fig 9. Same as Figure 7, but for V-band.

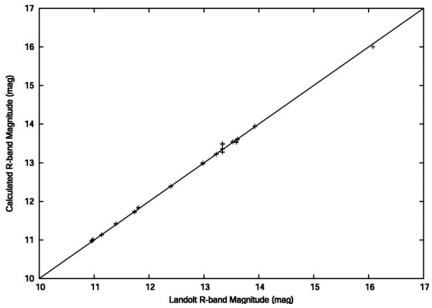

Fig 10. Same as Figure 7, but for R-band.

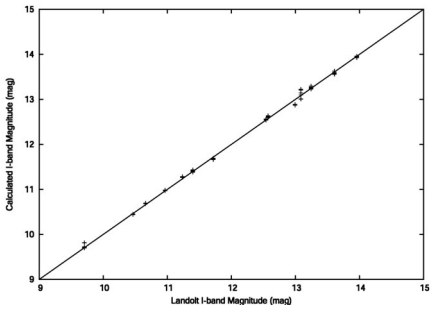

Fig 11. Same as Figure 7, but for I-band.

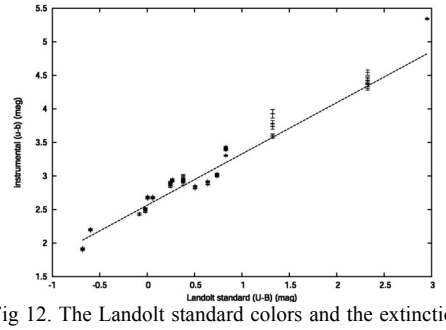

Fig 12. The Landolt standard colors and the extinction corrected instrumental colors are plotted for (U-B). The dotted straight line is the least-square fit of the data. The data were collected on 25 June, 2004.

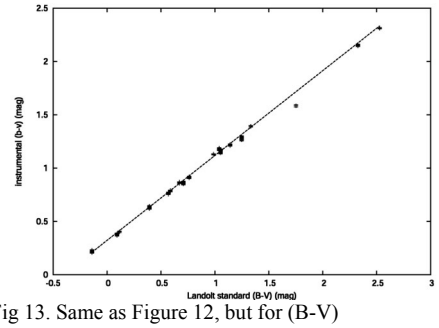

Fig 13. Same as Figure 12, but for (B-V)

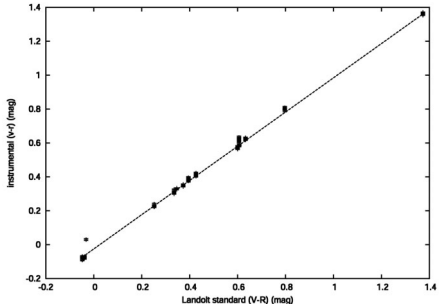

Fig 14. Same as Figure 12, but for (V-R)

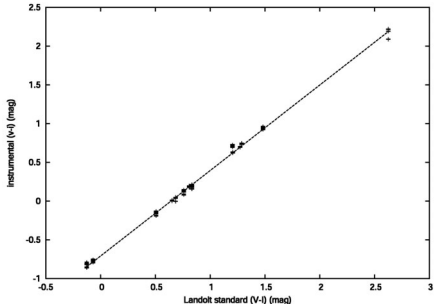

Fig 15. Same as Figure 12, but for (V-I)

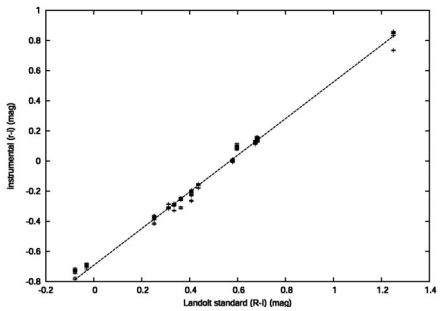

Fig 16. Same as Figure 12, but for (R-I)

total throughput of the telescope and instrument including telescope optics, filter transmittance and detector quantum efficiency.

The energy coming into the circle with the diameter of D outside the Earth's atmosphere from the star of magnitude m_λ per second is expressed as

$$E_\lambda = F_\lambda 10^{-0.4 m_\lambda} \pi \left(\frac{D}{2}\right)^2 \Delta\lambda \qquad (15)$$

Here, F_λ is the flux of a 0 magnitude star at wavelength λ, and $\Delta\lambda$ is the half-width of the filter. The number of incoming photons N_{photon} are calculated as

$$N_{calc} = \frac{E_\lambda}{h\nu} = \frac{E_\lambda \lambda}{hc} \qquad (16)$$

Here, h is the Planck constant, and c is the the light speed. The extinction corrected count rate of the CCD N_{obs} is expressed as

$$N_{obs} = \frac{C_{raw}}{T_{\exp}} 10^{-0.4kX} G \qquad (17)$$

Here, C_{raw} is the integrated raw count of the star, T_{exp} is the exposure time, k is the first-order extinction coefficient, X is the airmass, and G is the gain of the CCD. We define the total throughput E as

$$E = \frac{N_{obs}}{N_{calc}} \qquad (18)$$

The results are summarized in Table5. Since the transmittance of the U-band filter is unknown, we assumed a typical value. Results for both the slow and fast readout modes have good agreement.

Table 5. The total throughput for UBVRI bands including telescope optics, filter transmittance and quantum efficiency of the detector are summarized. Since the transmittance of the U-band filter is unknown, we assumed typical value.

Date	U	B	V	R	I	Remarks
17/Feb/2004	8%	27%	55%	47%	20%	fast readout
24/Jun/2004	7%	26%	53%	45%	19%	slow readout
25/Jun/2004	6%	27%	54%	47%	20%	slow readout

5.2 Sky Background Brightness

The brightness of the night sky was measured using the data taken on 24, 25 June, 2004. It was 6 and 7 days after the new moon, respectively. The Moon was almost going to set on 24 June, and the elevation was 4.0 to -0.5 degree above the horizon. On 25 June, the elevation of the Moon was 22.3 to 11.0 degree above the horizon. We have selected four-minute single exposures on 24 June and five-minute single exposures on 25 June for UBVRI bands. The angular separations between the moon and target field on 24 and 25 June are 65 and 53 degrees, respectively. The airmasses were 1.17 to 1.26 on 24 June, and 1.13 to 1.22 on 25 June. The correction for the airmass was applied using the formula (Krisciunas & Schaefer, 1991)

$$B_0(Z) = B_{zen} 10^{-0.4k(x-1)} x \qquad (19)$$

where

$$x = \left(1 - 0.96 \sin^2 Z\right)^{-0.5} \qquad (20)$$

Here, $B_0(Z)$ is the night sky brightness at zenith distance Z, B_{zen} is the night sky brightness at zenith, k is the extinction coefficient. We measured mean background level using the software “source extractor". The derived instrumental magnitudes and colors were converted into the standard system using the coefficients in Table 3. The color terms are taken into account. The background brightness levels of UBVRI bands on 24 June, 2004 are U=21.78±0.30, B=22.01±0.08, V=21.28±0.06, R=20.91±0.05, I=19.40±0.06 mag arcsec^{-2}, respectively. On 25 June 2004, they were U=21.03±0.20, B=21.22±0.06, V=20.83±0.04, R=20.59±0.05, I=19.47±0.05 mag arcsec^{-2},

respectively. The values we obtained at Lulin were compared to those of major ground based astronomical observatories in Table 6. Although the night sky brightnesses for B and V-band are roughly 0.8 and 0.5 magnitude brighter than major astronomical sites, it seems to be typical in East Asian region. Lin (1994) reported the dark time night sky brightness at Lulin as B=21.22 and V=20.72 mag arcsec^{-2} which are brighter than this work. This may suggest the variability of the brightness of the sky at Lulin due to the light pollution from nearby cities.

Table 6. The dark time night sky brightness for UBVRI bands measured at major ground based observatories are summarized. The brightness of the night sky is expressed in the unit of mag arcsec^{-2}.

Site	U	B	V	R	I	Ref.
Calar Alto	22.2	22.6	21.5	20.6	18.7	Leinert et al., 1995
Kiso		22.1	21.2	19.9	18.7	Ito, 1998b
Kitt Peak		22.9	21.9			Pilachowski et al., 1989
La Palma	22.0	22.7	21.9	21.0	20.0	Benn & Ellison, 1998
La Silla		22.8	21.7	20.8	19.5	Mattila et al., 1996
Lulin	21.8	22.0	21.3	20.9	19.5	This work
Mauna Kea		22.8	21.9			Krisciunas, 1997
Paranal	22.3	22.6	21.6	20.9	19.7	Patat, 2003
Tololo	22.0	22.7	21.8	20.9	19.9	Walker, 1987
Xinglong			21.0			Liu et al., 2003

5.3 Limiting Magnitude

We estimated the limiting magnitudes of LOT and PI1300B photometric system at Lulin. We used readout noise and dark current generation rate and sky back ground brightness estimated in this work. We adopted the CCD equation of the form

$$\frac{S}{N}=\frac{N_{star}}{\sqrt{N_{star}+n_{pix}\left(N_{sky}+N_{dark}+N_{readout}^{2}\right)}} \quad (21)$$

Derived limiting magnitudes for slow readout mode are U=19.7, B=21.4, V=21.2, R=21.1, and I=19.9 mag for the signal-to-noise ratio of 10 under the integration time of 300 sec and the aperture size of 3 arcsec.

6. Summary

The performance of the LOT and VersArray:1300B CCD photometric system at Lulin Observatory of the Institute of Astronomy at National Central University was evaluated. We have found the variability on the bias level when the fast-readout mode is used. The gain of the CCD is different for slow and fast readout. The transformation coefficients and the relation of instrumental and standard colors are derived. The extinction coefficients at Lulin on relatively dry nights are competitive to major astronomical sites. The total system performance was also measured. The night sky brightnesses seems to be typical values for observatory in East Asia region.

Acknowledgement

We would like to express our hearty thanks to Mr. Shih Jun-Shiung, Mr. Du Jing-Chuan, Mr. Shih Hao-Wei, and Mr. Wan Zong-Jing for their local supports at Lulin Observatory. We also thank Mr. Chang Ming-Shin, Mr. Urata Yuji, Miss Li Yang-Shyang for their help for the observations. Kinoshita, D. thanks to the fellowship from the Japan Society for Promotion of Science (ID: 15-1-2-02681-1).

Reference

Benn, D. R., Ellison, S. L., 1998, *New Astronomy Reviews*, 42, 503.

Chang, M.-S., 2004, "*Annual Report of Lulin Observatory*"(in Chinese), edited by Chang, M.-S., p.14.

French, L. M., Morales, G., Dalton, A. S., Klavetter, J. J.,Conner, S. R., 1985, *AJ*, 90, 668.

Giacconi, R., Gilmozzi, R., Leibundgut, B., Renzini, A.,Spyromilio, J., Tarenghi, M., 1999, *A&AL*, 343, 1.

Guerrero, M. A., Garcia-Lopez, R. J., Corradi, R. L. M., Jimenez, A., Fuensalida, J. J., Rodriguez-Espinosa, J. M., Alonso, A., Centurion, M., Prada, F., 1998, *New Astronomy Reviews*, 42, 529.

Hanuschik, R., 2004, http://www.eso.org/observing/dfo/quality

Henden, A. A., Kaitchuck, R. H., 1990, "*Astronomical Photometry*", Willmann-Bell, Inc., p. 322.

Howell, S. B., 2000, "*Handbook of CCD Astronomy*", Cambridge University Press

Huang, Y.J., Lee, C.C., Chen, W.P., 2004, "*Annual Report of Lulin Observatory*", Edited by Chang, M.S., p. 47.

Ito, N., 1998a, "*Observation of Photometric Standard Stars*" in the Internal Report of Kiso Observatory (in Japanese).

Ito, N., 1998b, *"Estimation of the Limiting Magnitude of 2KCCD Camera*" in the Internal Report of Kiso Observatory (in Japanese).

Kinoshita, D., Huang, K.Y., Wu, Y.L., Chang, Y.S., Urata, Y., 2004, "*Annual Report of Lulin Observatory*", Edited by Chang, M.S., p. 30.

Krisciunas, K., 1997, *PASP*, 109, 1181.

Krisciunas, K., Schaefer, B., 1991, *PASP*, 103, 1033.

Krisciunas, K., Sinton, W., Tholen, D., Tokunaga, A., Golisch, W., Griep, D., Kaminski, C., Impey, C., Christian, C., 1987, *PASP*, 99, 887.

Landolt, A. U., 1992, *AJ*, 104, 372.

Leinert, C., Vaisanen, P., Mattila, K., Lehtinen, K., 1995, *A&ApS*, 112, 99.

Lin, H.C., 1994, "*Measurements of Night Sky Brightness using Open Cluster M44 at Lulin Observatory*", master thesis at National Central University of Taiwan (in Chinese).

Liu, Y., Zhou, X., Sun, W.H., Ma, J., Wu, H., Jiang, Z.J., Xue, S.J., Chen, J.S., 2003, *PASP*, 115, 495.

Mattila, K., Vaisanen, P., Appen-Schnur, G.F.O. v., 1996, *A&AS*, 119, 153.

Miller, R., Osborn, W., 1996, *IAPPP Communications*, 63, 40.

Motohara, K., Iwamuro, F., Maihara, T., Oya, S., Tsukamoto, H., Imanishi, M., Terada, H., Goto, M., Iwai, J., Tanabe, H., Hata, R., Taguchi, T., Harashima, T., 2002, *PASJ*, 54, 315.

Nakos, T., Sinachopoulos, D., van Dessel, E., 1997, *A&AS*, 124, 353.

Patat, F., 2003, *A&A*, 400, 1183.

Pilachowski, C., Africano, J. L., Goodrich, B. D., Binkert W., 1989, *PASP*, 101, 707.

Princeton Instruments, Inc., www.princetoninstruments.com.

Stone, R. P. S., Baldwin, J. A., 1983, *MNRAS*, 204, 347.

Sung, H.K., Bessell, M. S., 2000, *PASA*, 17, 244.

Tan, H.S., Zhang, B.-R., 1999, in the proceedings of the 4th East Asian Meeting on Astronomy (4th EAMA) "*Observational Astrophysics in Asia and its Future*", Edited by Chen, P.S., p. 18.

Waker, A., 1987, *NOAO Newsletter*, 10, 16.

Yan, H.J., Burstein, D., Fan, X.H., Zheng, Z.Y., Chen, J.S., Byun, Y.I., Chen, R., Chen, W.P., Deng, L.C., Deng, Z.G., Fang, L.Z., Hester, J.J., Jiang, Z.J., Li, Y., Lin, W.P., Lu, P., Shang, Z.H., Su, H.J., Sun, W.H., Tsay, W.S., Windhorst, A., Wu, H., Xia, X-Y.,Xu, W., Xue, S.J., Zheng, Z., Zhu, J., Zou, Z.L., 2000, *PASP*, 112, 691.